Regular Research Manuscript

MPPT DC-DC Buck-Boost Converter for Off Grid Hybrid Solar-Wind-Battery System in Ikuza Island, Tanzania

Nassoro S. Nassoro[1,2], Consalva J. Msigwa[2], Aviti T. Mushi[1†] and Bakari M. M. Mwinyiwiwa[1]

[1]Department of Electrical Engineering, University of Dar es Salaam, Tanzania

[2]Department of Electrical Engineering, Dar es Salaam Institute of Technology, Tanzania

†Corresponding author: aviti.thadei@udsm.ac.tz, aviti.bahati@gmail.com

ORCID: https://orcid.org/0000-0002-2958-2919

ABSTRACT

Ikuza Island in Kagera-Tanzania faces lack of electricity due to cost challenges of extending the grid by marine cables and other transmission facilities. These makes such endeavour not appealing to the supply authority due to those higher charges. Therefore, this paper undertakes to design hybrid renewable energy sources for the island by specifically focusing on the buck-boost converter for the energy conversion from these renewable resources. The design of the bidirectional buck-boost converter for maximum power point tracking in off-grid hybrid renewable energy systems is multifaceted due to the inhomogeneity nature of the renewable energy sources. The bidirectional buck-boost converter, solar PV, wind-based generator, and energy storage system are designed and simulated in MATLAB/Simulink software. The designed system is tested with varying solar irradiance (750 to 1000 W/m^2), temperature (20 to 25 ℃) and wind speed (150 to 157.5 radians/s) at constant load of 260 A while load variation involved varying the load current from 0 to 260 A at solar irradiance, temperature, and wind speed of 1000 W/m^2, 25 ℃ and 157.5 radians/s, respectively. The variation of DC link bus voltage at different load conditions is reported. The simulation results show that the designed converter is able to maintain DC link voltage at 600 V. Moreover, the DC link voltage shows a maximum drop of approximately 0.67% during the constant load condition. Contrarily, a significant improvement is observed when the designed converter operates with the hybrid system of solar PV, PMSG-based wind generator and with energy storage system.

Keywords: *Hybrid renewable system, Bidirectional buck-boost converter, MPPT algorithm, Ikuza Island*

INTRODUCTION

Electricity plays a crucial role in the socioeconomic development of any society. A large proportion of electrical energy generation is currently dominated by fossil fuel such as coal, natural gas, and hydrocarbon oils (Garcia et al., 2017; Nyanda et al., 2022). These fuels have significant hydrocarbon footprints, which are harmful to the environment (Anish John Paul et al., 2021; Garcia et al., 2017). Due to the negative effects of fossil fuels, it is essential that nations rely more on utilizing energy from renewable sources as a necessary replacement source for fossil fuels (Minja & Mushi, 2023; Raj & Praveen, 2022).

Solar and wind energy are the most promising renewable energy sources for meeting ultra-clean energy demand, especially in remote areas where grid extension is impractical. Its inherent advantages over other renewable energy resources include reduced maintenance, safe operation, ample availability, and easy manageability (Chilumba et al., 2023; Uthirasamy et al., 2022). However, these renewable energy sources are inherently intermittent and frequently provide less power than non-renewable sources (Juma et al., 2021a; Juma et al., 2021b; LakshmanRao et al., 2014). As a result, to provide reliable and sustainable energy, a method of combining various sources (hence called hybrid sources) is required. In contrast to a single-source system, a hybrid renewable energy system combines multiple renewable energy sources to provide continuous electricity to customers. This hybrid renewable energy source plays a crucial role in generating power in disadvantaged areas where grid extension is not feasible, such as in isles or remote areas (Barone et al., 2021; Cabrera et al., 2018; Minja & Mushi, 2022). Besides, this hybrid renewable energy source is critical to the achievement of the sustainable development goals (SDGs) and enhance living standard consequently.

In recent decades, efforts have been made on utilizing the hybridization of renewable energy systems. In the hybridization, solar and wind act as the primary energy sources while fuel cell and battery energy storage system act as back-up systems. The hybridization of renewable energy system makes the energy mix affordable for economic activities particularly in remote or islands, of which majority of their residents are low-income earners. The cost of generating electricity on islands can be up to ten times that of the mainland. This situation is undoubtedly a financial burden for the islanders. To date, islands around the world face significant energy supply issues, with oil products controlling their energy mix (Fungo et al., 2021; Kaldellis, 2021). In many cases, oil has had a negative impact on the island energy security, economy, environment, and social development (Cabrera et al., 2018; Hajjaji et al., 2022). Many researchers and policymakers are interested in the hybridization of renewable energy on islands because islands are interesting test fields (Cabrera et al., 2018; Kapsali & Anagnostopoulos, 2017). Tilos Island of Greek is mentioned as the first in the Mediterranean to be fully powered by wind-solar hybrid system (Kapsali & Anagnostopoulos, 2017). Further, Samso island in Denmark replaced its fossil fuels by renewable energy resources. The paper by Hajjaji et al. (2022) optimized the dimension of the PV-wind-battery-hydraulic generation system for a remote island in Tunisia. Kalamaras et al. (2019) proposed a hybrid PV system-wind-electrolyzer-hydrogen-fuel cell-battery off grid DC system to meet the electric and thermal demand of a typical household in Hydra, a Greek Island.

The optimum design of the hybrid system consisted of a 3.35 kW PV system, 3 kW wind turbine, 2.9 kW fuel cell, 6 batteries, 4.2 kW electrolyser and a hydrogen tank of 70 kg. Paper by See et al. (2022) evaluated four hybrid systems with diesel generator-PV-wind-battery

in a remote community on Malawali Island in Sabah, Malaysia. They determined which source had the lowest electricity costs. To achieve the best technical, financial, and environmental results, the design included a 50 kW diesel generator, a 12.4 kW PV, 11.1 kW wind turbines, and 18 batteries. This paper by Khan et al. (2014) modelled a wind-PV-diesel generator-battery-tidal system to provide affordable electricity at Sandwip Island, in Bangladesh. That research revealed that the cost of electricity is minimum (0.069 $/kWh) for wind-PV-diesel and maximum (0.088 $/kWh) for tidal-wind-PV-diesel systems. Despite the efforts of adopting hybrid renewable energy and comparable number of islands in the globe, it's only 1% of the islands that has sufficient electrical energy (Kaldellis, 2021). Furthermore, with the existing hybrid renewable energy system, insufficient electricity is generated that could not electrify large island's population. This can be partly attributed to poor converter designs, which primarily result in inefficient power conversion. However, Sub-Saharan African (SSA) nations continue to have slow electrification rates (Irechukwu & Mushi, 2020). The situation is made even worse when accounting for the lack of prevalence of hybrid renewable energy systems in islands. Tanzania is one of the SSA nations with several islands, and she struggles with the high price of fossil fuel electricity. In order to lessen its reliance on fossil fuels, Tanzania's government has adopted a hybrid renewable energy system for applications that are sustainable (Marcel et al., 2021). Therefore, having DC-DC converters for high voltage conversion when considering the adoption of a hybrid renewable energy system in islands could be advantageous for widespread electricity access.

In this study, a design and simulation of the DC-DC converter with MPPT algorithm for off grid hybrid solar-wind-battery system at Ikuza Island, Tanzania is undertaken. The main contributions of this study include:

a) To design the DC-DC converter that receive the uncontrolled DC voltage from the solar-wind-battery system and convert an average DC voltage of up to 600 V DC to feed the Ikuza Island electrical load demand.

b) To assess the performance of the DC-DC converter by investigating the average output DC voltage of the DC-DC converter under different load conditions.

METHODS AND MATERIALS

Description of Study Area

The isles area targeted for this study is Ikuza Island, also known as Igusa Island. The island is in Kagera Region, Tanzania, East Africa, having an estimate terrain elevation above sea level of about 1,135 m. Its coordinates are 2°7'60" S latitude and 31°46'0" E longitude. The island covers a total area of 80 km² with six villages. Its popular activities include tourism, indigenous system of farming, fishing and several small-scale enterprises. As of now, the island is considered as a disadvantaged area for grid connection despite a large number of economic activities. The electricity price in Ikuza Island is high due, in part, to a reliance on diesel for its power generation and inefficient ways of transmitting and distributing electricity. Besides, the generated electricity could largely be unreliable, caused by long overdue maintenance being carried out on the city's diesel chugging generators leading to power outages. To improve the reliability and cost of power in Ikuza Island to boost economic activities and living standards, consequently, renewable energy sources could be an alternative way to achieve the target.

Renewable Energy Potential at The Targeted Area

Ikuza Island has plentiful resources of renewable energy including solar and wind energy. Table 1 shows the solar radiation data at Ikuza Island. The solar data listed in Table 1 were extracted from Global Solar Atlas (GSA,

2023). The solar radiation data in Table 1 is useful for estimating the PV energy potential. Figure 1 shows the average monthly solar energy generation in kWh/m²/day on optimum tilted surface at 6°.

To further understand solar behaviour of the targeted area, extra yearlong solar data were gathered from the NASA database (NASA, 2023) for the year 2021 and are summarized in Table 2. From Table 2, the highest temperature is 23.9 °C while the minimum is 18 °C. The sky clearness index ranges from 0.6 to 1, reflecting the higher possibility of harvesting the solar energy in the targeted area. From Figure 1 it is observed that the worst month for photo voltaic generation is July having an energy generation from solar radiation of 6.38 kWh/m²/day. Despite the lower sunshine hours, however, the sky remains to be clear, indicating the potential for solar energy harvest. The hours for daily peak energy generation beyond 350 kWh/m² range from 12:00 pm to 16:00 pm.

The wind data, average monthly wind speed at the targeted area is depicted by Figure 2. It is observed that the minimum wind speed reach 7.32 m/s in November followed by January and February with 7.47 m/s and 7.73 m/s respectively.

Estimation of Load Requirement

To ensure that the estimated power generation meets the demand, load estimation need to be properly undertaken. For this study, the electrical loads at the targeted area, their categories, power ratings, quantities and operating hours were studied and summarized as presented in Table 3. The village has a total of 237 households. It is observed that the categories of electrical loads are mainly small and medium domestic houses, commercial centres, schools, dispensary, and religious houses. It can further be seen that schools have higher wattage lamps but fewer working hours while the rest have lower wattage lamps with longer working hours.

Table 1: Solar radiation data at Ikuza island, Kagera region

Map data	Per day	Per year
Specific PV power output	4.471 kWh/kWp	1631.9 kWh/kWp
Direct normal irradiation	4.578 kWh/m²	1670.9 kWh/m²
Global horizontal irradiation	5.569 kWh/m²	2032.6 kWh/m²
Diffuse normal irradiation	2.260 kWh/m²	825.0 kWh/m²
Global tilted irradiation at opt. angle	5.595 kWh/m²	2043.2 kWh/m²
Optimum tilt of PV modules	6/0º	6/0º
Maximum air temperature	23.0 ºC	23.0 ºC
Minimum air temperature	20.0 ºC	20.0 ºC
Humidity	75%	89%
Terrain elevation	1238 m	1238 m

Table 2: Average yearlong data in the study area collected in 2021

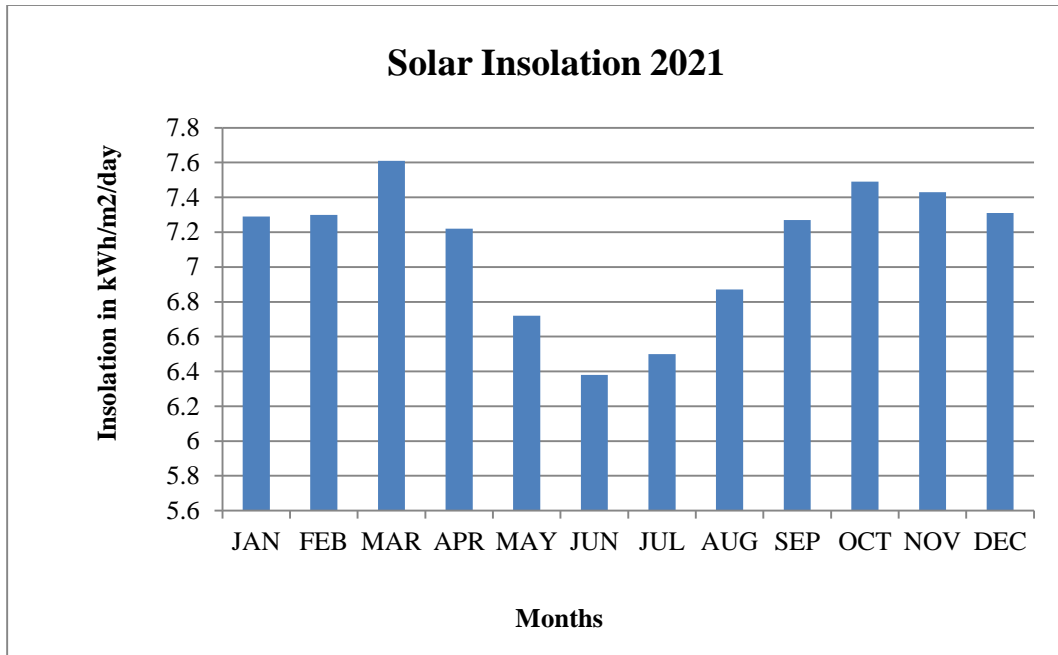| Parameters	J	F	M	A	M	J	J	A	S	O	N	D
Temperature (˚C)	22	23.9	22	21	20	19	18	19.7	22	24	20	23
Sky Clearness Index	1	0.8	0.9	0.9	0.7	1	0.9	0.88	0.7	0.7	0.6	0.8
Reflected Solar Radiation (kWh/m²/day)	4	5	4	4	5.4	6	5.6	6.61	6.6	6.8	5.53	5
Global Solar Radiation (kWh/m²/day)	6	6	6	5	5.5	6	5.6	6.34	6.7	7	6.42	6.1
Diffuse Solar Radiation (kWh/m²/day)	3	3	3	3	2.1	2	2	1.84	2	2	2.48	2.6

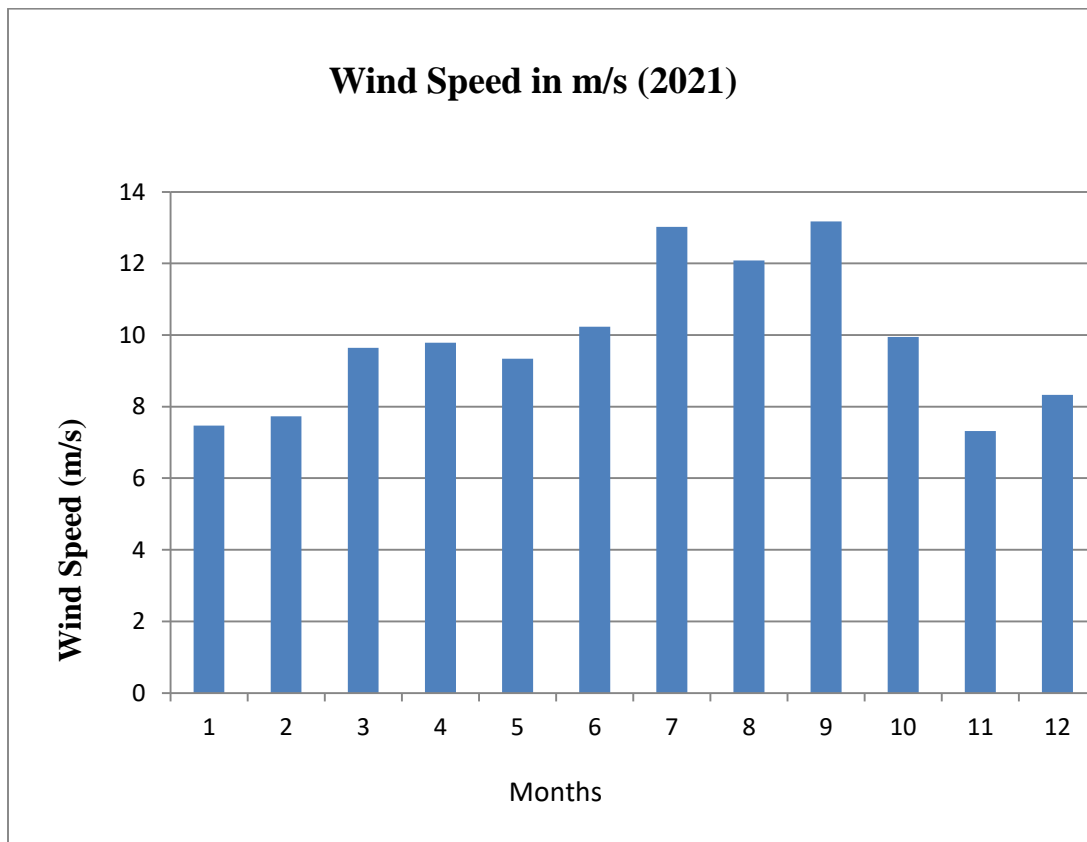**Figure 1: Average monthly solar energy generation in kWh/m²/day.**

Figure 2: Estimated wind speed in Ikuza Island.

Modelling of Solar Cell and PV Module

The electrical equivalent circuit of a solar cell is represented by a one-diode model as depicted in Figure 3 (Justo & Mushi, 2020), where the current I_D represents the diode current also called dark current, I_{ph} a photocurrent source of a diode, and R_s a series resistance, which represents the resistance within each cell and between cells. The difference between the photocurrent and the normal diode current gives the net current (I) that flows out of the solar PV cell as shown in Equation (1). The solar saturation current is represented by I_0, terminal voltage is V, shunt resistance of the solar cell is R_{sh}, diode ideality factor is m, Boltzmann constant is k, cell temperature is T_C,

and charge is q. Solar cells are typically organized into modules which are encased in various case materials to protect the cells and electrical connectors from the harsh environment. The PV cells in modules are strung in N_{PM} parallel branches, each with N_{SM} solar modules in series, as shown in Figure 3b. The sun's radiated energy on the surface of PV modules is converted to electrical power (P_t^{PV}) at hour t, given by Equation (2).

The A_{PV} is the area of one solar PV module, S_t^{IP} is the predicted solar irradiance, S_{PR} is solar system performance ratio (typically 0.9 or 90%), S_{PY} is the solar panel yield, and Δt is the step time (1 hour in this study). The total time for the period of interest is depicted by T.

Table 3: Electrical load requirement for 237 households

Category	Load	Quantity per household	Power (kW) Per household	Per village	Working hours (h)	Daily energy requirement (kWh/day)
Small domestic house	5 W LED lights	5	0.025	16.175	12	194.1
	4 W Radios	1	0.004	2.588	5	12.94
	Phone chargers	1	0.005	3.235	5	16.175
Medium domestic house	5 W LED lights	9	0.045	10.665	12	51.8319
	8 W Radios	1	0.008	1.896	3	0.045504
	50 W LED TV	1	0.05	11.85	5	2.9625
	Phone chargers	1	0.005	1.185	5	0.029625
Commercial centres/shops	9 W LED lights	5	0.045	0.585	12	7.02
	50 W LED TV	1	0.05	0.65	4	2.6
	32 W Music system	1	0.032	0.416	16	6.656
	130 W Fridge	1	0.13	1.69	5	8.45
	Phone chargers	1	0.005	0.065	12	0.78
Primary schools	20 W LED lights	32	0.64	0.64	2	1.28
	20 W LED lights	7	0.14	0.14	1	0.14
	80 W Computer	3	0.24	0.24	3	0.72
	Phone chargers	1	0.005	0.005	3	0.015
Secondary schools	20 W LED lights	20	0.64	0.64	5	3.2
	20 W LED lights	7	0.14	0.14	2	0.28
	80 W Computer	3	0.24	0.24	3	0.72
	Phone chargers	1	0.005	0.005	3	0.015
Dispensary	11 W LED lights	9	0.099	0.099	5	0.495
	20 W LED lights	7	0.14	0.14	12	1.68

Tanzania Journal of Engineering and Technology (Tanz. J. Engrg. Technol.), Vol. 42 (No. 3), Oct. 2023

176

Category	Load	Quantity per household	Power (kW)		Working hours (h)	Daily energy requirement (kWh/day)
			Per household	Per village		
Small domestic house	5 W LED lights	5	0.025	16.175	12	194.1
	4 W Radios	1	0.004	2.588	5	12.94
	Phone chargers	1	0.005	3.235	5	16.175
	20 W Microscope	1	0.02	0.02	1	0.02
	1.5 kW Autoclave	1	0.011	0.011	1	0.011
	10 W Centrifuge	1	0.011	0.011	1	0.011
	Phone chargers	4	0.02	0.02	5	0.1
Mosques	11 W LED lights	21	0.231	0.231	12	2.772
	90 W PA system	1	0.09	0.09	2	0.18
	Phone chargers	5	0.025	0.025	5	0.125
Churches	11 W LED lights	18	0.198	0.198	12	2.376
	60 W Piano	1	0.06	0.06	6	0.36
	90 W PA system	1	0.09	0.09	2	0.18
	Phone chargers	4	0.02	0.02	5	0.1
					Total	**318.370529**

$$I = I_{ph} - I_o\left(\exp\left(\frac{q(V + IR_S)}{mkT_C}\right) - 1\right) \quad (1)$$

$$P_t^{PV} = A_{PV} S_t^{IP} S_{PR} S_{PY} N_{PV} \Delta t \quad (2)$$
$$\forall t \in T$$
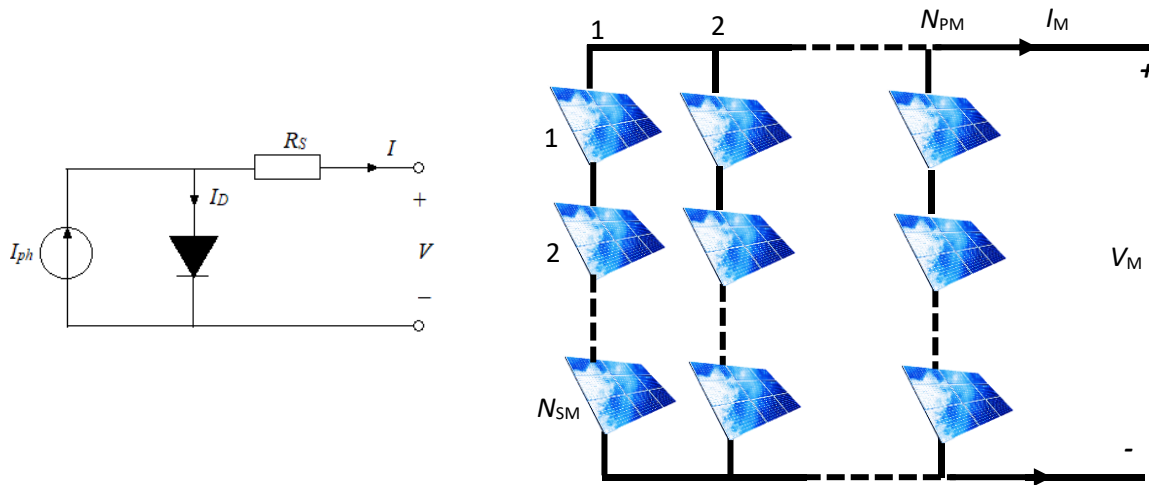
Figure 3: A representation of (a) solar cell circuit and (b) solar PV module strings.

Modelling of Wind Turbine

Permanent magnet synchronous generators (PMSG) with direct drives and no gearboxes are popular for wind turbine applications. This is due to them being highly efficient and requires little upkeep. For these reasons, PMSG is preferred for standalone systems (Badwawi et al., 2015). To deploy these advantages, the current study employed PMSG coupled to a wind turbine. The mathematical model of PMSG can be described in the d-q reference system as shown in Equations (3) - (5). The d-q axes currents and voltages are i_{sd}, i_{sq}, u_{sd}, and u_{sq}, respectively. The stator angular speed is w_s. The PMSG inductances are L_{sd} and L_{sq}. The flux in the stator is φ_p with the stator resistance of denoted as R_{sa} and number of poles is P. The electromagnetic torque is T_e in Equation (5).

$$\frac{di_{sq}}{dt} = -\frac{R_{sa}}{L_{sq}} i_{sq} + \omega_s \left(\frac{L_{sd}}{L_{sq}} i_{sd} + \frac{1}{L_{sq}} \varphi_p \right) u_{sd} + \frac{1}{L_{sq}} u_{sq} \tag{3}$$

$$T_e = 1.5 \left(\frac{P}{2} \right) \left[\varphi_p i_{sq} + i_{sd} i_{sq} \left(L_{sd} - L_{sq} \right) \right] \tag{4}$$

$$\frac{di_{sd}}{dt} = -\frac{R_{sa}}{L_{sd}} i_{sd} + \omega_s \frac{L_{sq}}{L_{sd}} i_{sq} + \frac{1}{L_{sd}} u_{sd} \tag{5}$$
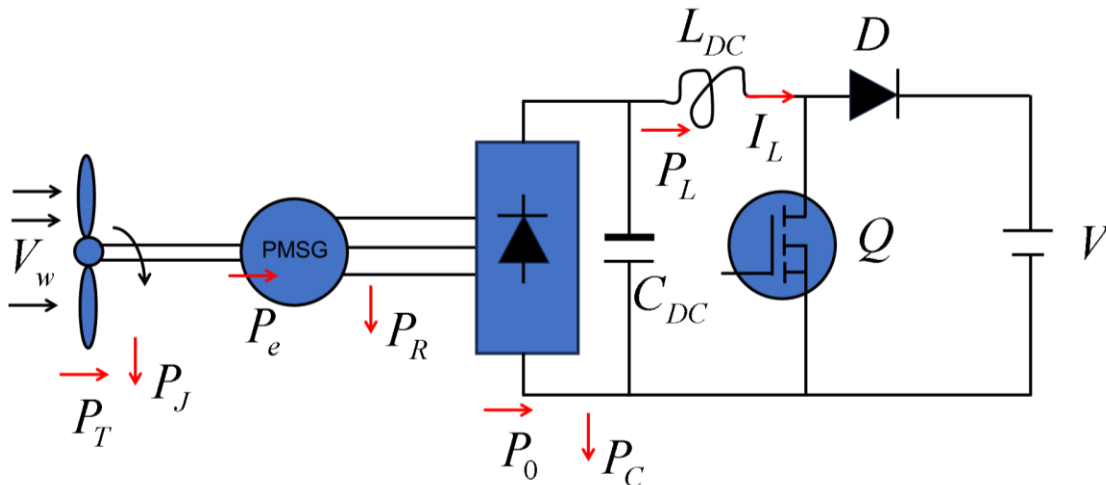

Figure 4: PMSG based wind turbine model with diode rectifier and converter showing the power distribution.

When the turbine is blown by the wind and friction losses are considered, the power captured by the wind turbine is represented by P_T. The PMSG absorbs the power, and the remainder (P_J) changes the shaft speed. As a result, the electromagnetic power P_e enters the PMSG. Without considering the machine's magnetic losses and the diode losses, this electromagnetic power divides into the resistive losses caused by the PMSG windings P_R and the diode bridge output power P_0. The majority of P_0 enters the boost converter as P_L and the remainder is used to charge the capacitor C_{DC} and is later seen as output V or V_b.

Tanzania Journal of Engineering and Technology (Tanz. J. Engrg. Technol.), Vol. 42 (No. 3), Oct. 2023
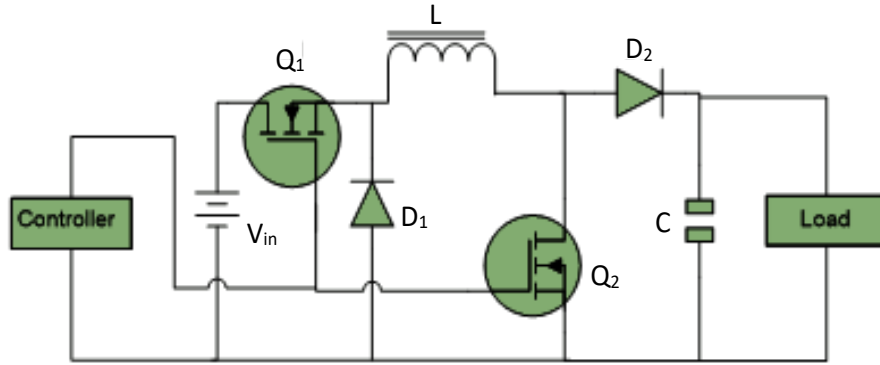
178

Figure 5: A buck-boost converter model with controller.

Modelling of a Buck-Boost Converter and Controller

The circuit of a buck-boost converter is depicted in Figure 5. The buck-boost converter can be modelled into two modes: buck and boost modes. During the buck mode, batteries are charged to voltage V_b, hence the duty cycle (D_1) can be expressed as shown in Equation (6). If the switching frequency (f_s) is 20 kHz, therefore, the charging inductor (L_{DC}) is calculated as shown in Equation (7). During the boost mode, the duty cycle (D_2) and charging inductor can be calculated as shown in Equations (8) and (9), respectively.

$$D_1 = \frac{V_b}{V_{dc}} \tag{6}$$

$$L_{DC} = \frac{D_1(V_{dc} - V_b)}{f_s \Delta I_L} \tag{7}$$

The ΔI_L is the variation of charging current (typically 20%).

$$D_2 = \frac{V_b - V_{dc}}{V_{dc}} \tag{8}$$

$$L_{DC} = \frac{V_b D_2}{f_s \Delta I_L} \tag{9}$$

To make sure that the DC link voltage is kept constant, a controller was designed (shown in Figure 5) to control the buck-boost converter. The designed controller ensures power flows continuously between the DC bus and the battery storage despite the variations in solar, wind or load variables.

Maximum Power Point Tracking Control

To further maximize the energy harvest, the maximum power point tracking (MPPT) technique is used. Despite the increased energy harvest, this technique effectively reduces energy costs because it tracks and capture the maximum power from solar PV. Usually, the MPPT controllers are driven by a set of algorithms to achieve the optimum performance. Among many algorithms deployed on MPPT control, an incremental conductance (INC) algorithm is simple, easy to implement, and is widely used to extract MPP. Moreover, it overcomes the disadvantages of the perturb and observe algorithms. Figure 7 shows the flowchart of MPPT based on incremental conductance algorithm employed in this study.
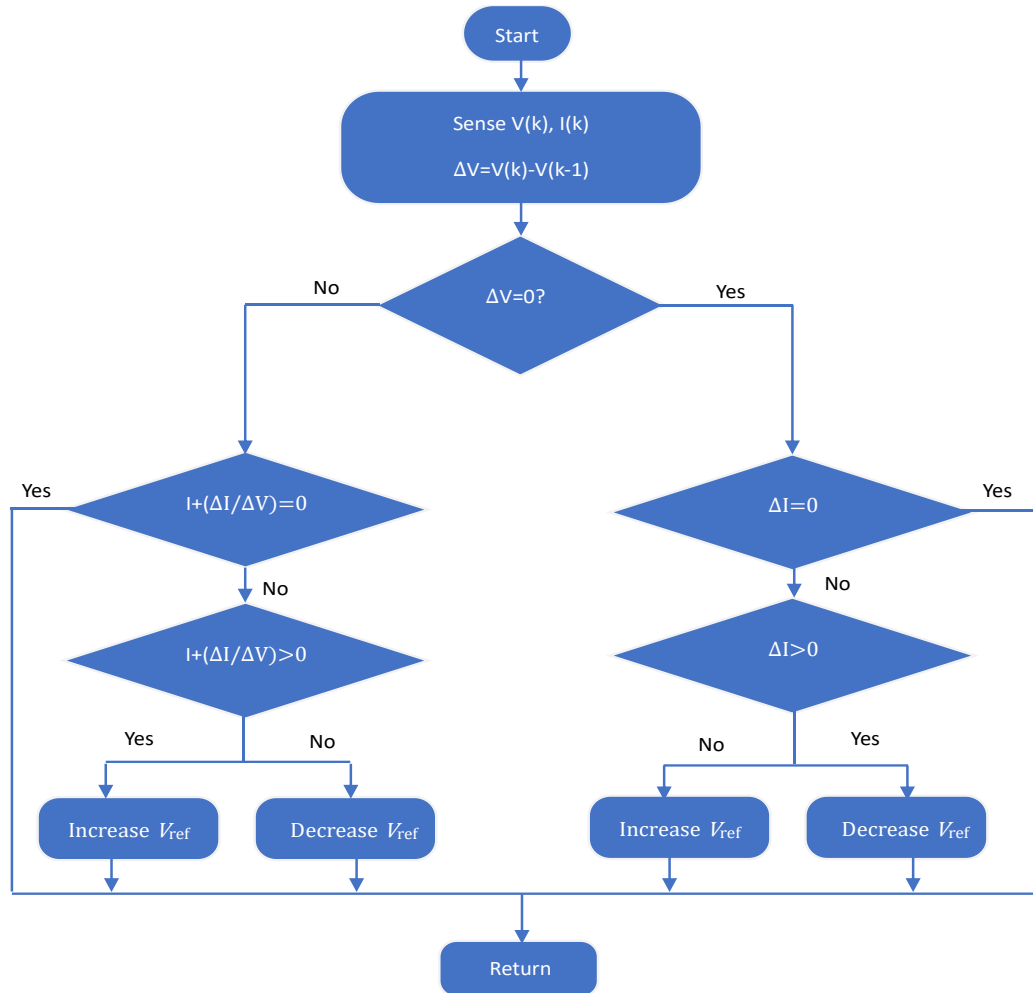
Figure 7: Flowchart of MPPT based on incremental conductance.

Simulation Procedure

The circuit diagram of the hybrid solar-wind-battery storage system is shown in Figure 8. The circuit was simulated on the MATLAB-Simulink R2018b software, and system parameters were inserted. Table 4 shows the values of the circuit parameters. Simulation was done by varying solar PV using MPPT with incremental conductance technique without a battery connected. Moreover, simulation is conducted with wind speed variations on a constant load. Later, hybrid system of solar PV, wind turbine, and battery energy storage system is simulated while the load is varied stepwise. The simulation used Apollo Solar Energy ASEC-300G6S when the solar irradiance was varied from 0.5 to 1.0 kW/m^2 at 25 °C the result is shown in Figures 9a-b. Also, I-V and P-V curves at temperatures of 16 to 30°C are shown in Figure 9c-d. Figure 9e shows the step variation of the load current.
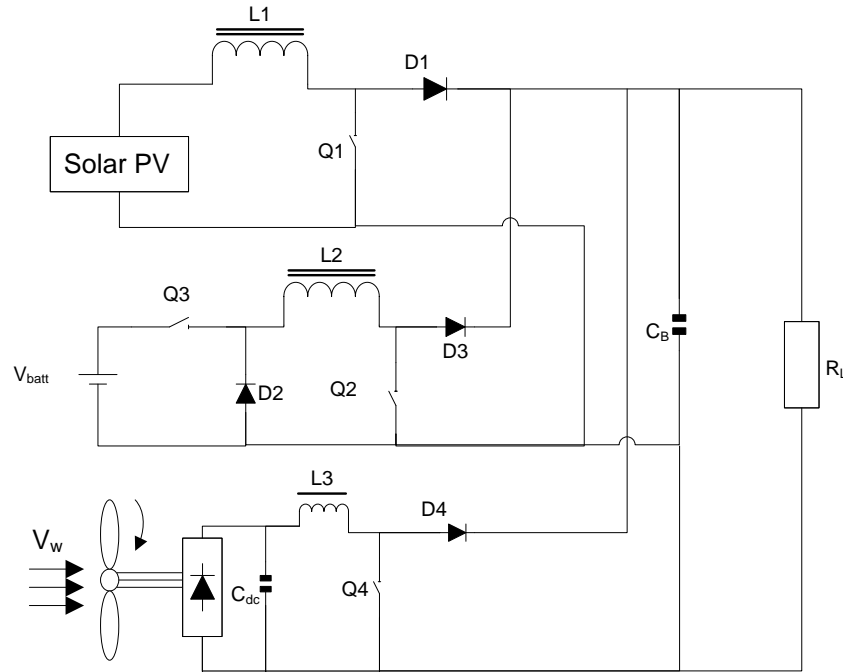
**Figure 8: Typical hybrid system configuration simulated in the current study.**

Table 4: Parameters used in simulation

| System	Section	Parameter	Variable	Unit	Value
Solar	PV module	Maximum power	P_m	W	300.0
		Voltage at max power point	V_{mp}	V	35.46
		Current at maximum power point	I_{mp}	A	8.46
		Cells per module	N_{cell}		72
		Open circuit voltage	V_{oc}	V	45.07
		Short circuit current	I_{sc}	A	8.91
		Temperature coefficient of V_{oc}	T_{cv}	%/deg.C	-0.343
		Temperature coefficient of I_{sc}	T_{ci}	%/deg.C	0.072896
Wind	PMSG	Rated Power		kW	5
		Rated Current		A	13.1
		Rated Voltage		V	220
		Stator Resistance		Ω	0.8654
		D-axis Inductance		mH	22.91
		Q-axis Inductance		mH	8.76
		No. of pole pairs			3
		Rated Speed		rpm	1000
	Wind turbine	Cut-in wind speed		m/s	2.5
		Rated wind speed		m/s	12
		Rotor Diameter		m	5.5
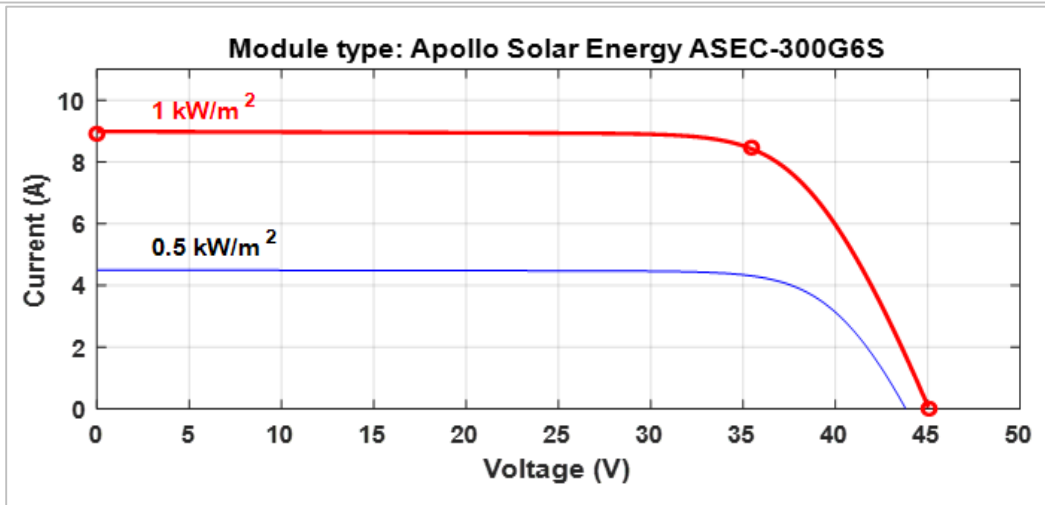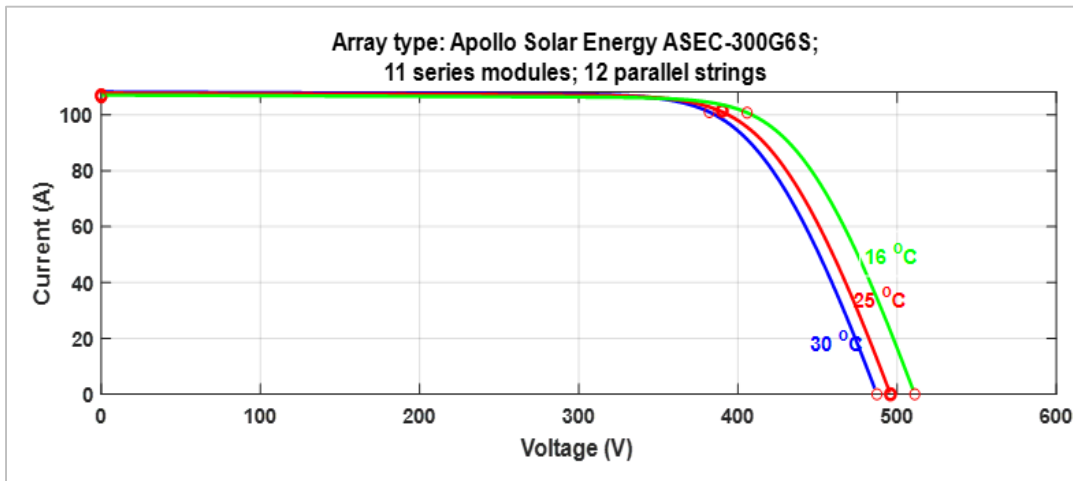
(a)
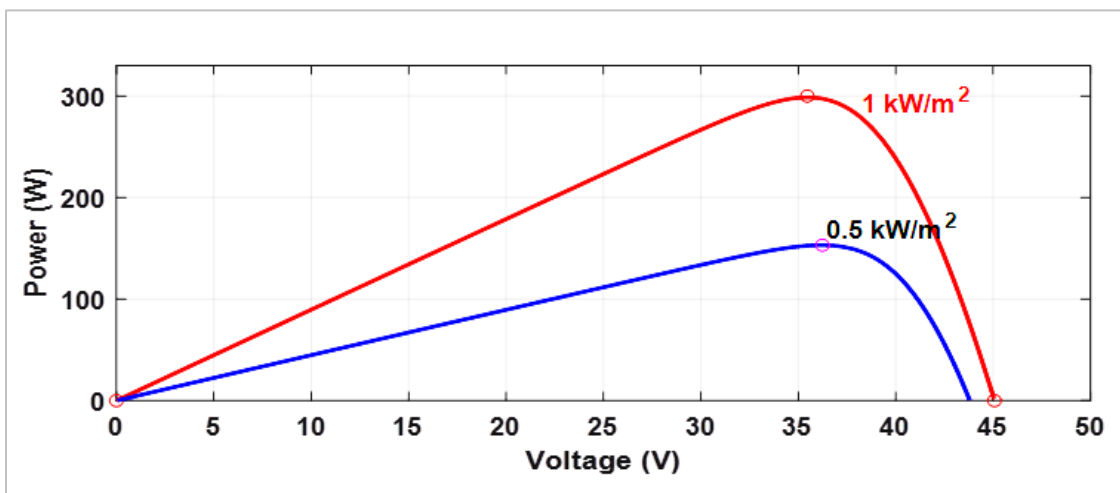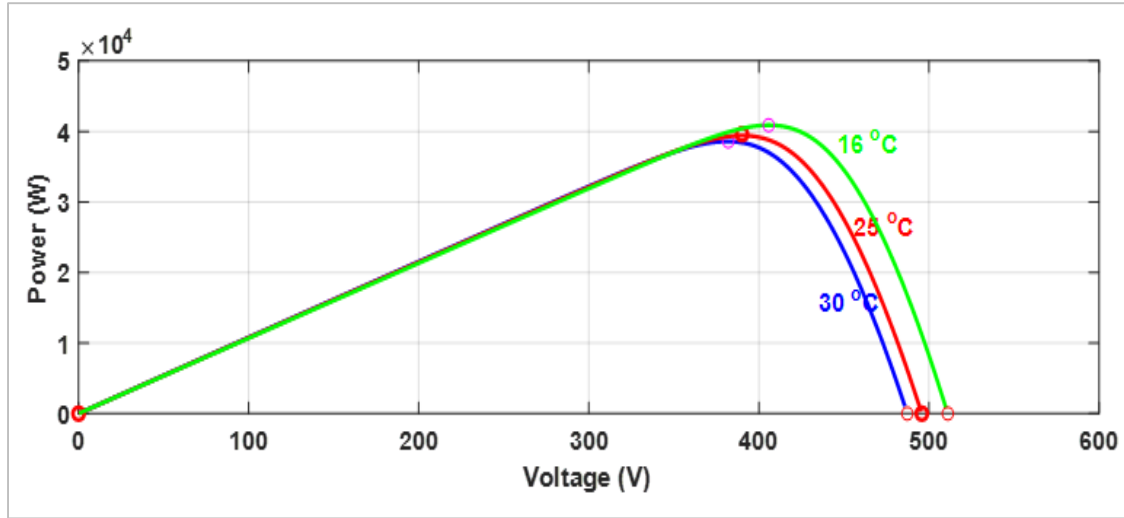
(b)
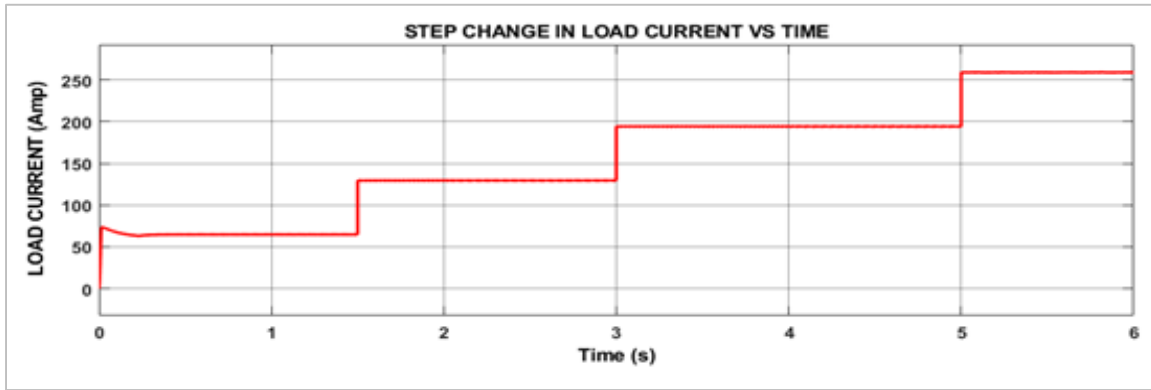
Figure 9: Verification results for: (a) I-V and P-V curves at 0.5 to 1.0 kW/m², (b) I-V and P-V curves at 16 to 30°C, and (c) step change in load current.

RESULTS AND DISCUSSION

Performance of the DC-DC Converter at Constant Load

According to the electrical demand shown in Table 1, there are 12 parallel solar panels that produce about 101.5 A and there are 11 series connected solar panels that produce a nominal voltage of 390.06 V. Consequently, the solar plant develops a nominal power of 40 kW at the DC bus. The solar irradiance in the targeted area ranges from 638 to 756 W/m², which made using the DC-DC boost converter important to increase solar PV voltage to the necessary DC

bus voltage at this solar irradiance using MPPT control. Therefore, the DC-DC boost converter maintained the V_{DC} to 600 V. Figure 9 shows the V_{DC} output by the DC-DC buck-boost converter when solar irradiance and temperature are varied from 1000 to 750 W/m² and 25 to 20 °C for about 2 seconds, respectively. The load was fixed at 250 A.

In Figure 9a, without energy storage system variation in solar irradiance (between 2 to 4 second) leads to drop in V_{dc} from 600 to 596 V between 4 and 6 second, solar irradiance was increased back to 1000 W/m² and the V_{DC} reached to 600 V. This change in V_{DC} is

approximately 0.67% which falls within the acceptable range. Between 6 to 8 seconds, the temperature was dropped from 25 to 20 °C while maintaining solar irradiance at 1000 W/m². It can be observed that the V_{DC} increases from 600 to 615 V.

To minimize rise time and voltage dips when the load or solar irradiance changes, the energy storage system is connected to the solar PV system using a buck-boost converter. The designed system was tested with varying solar irradiance (750 to 1000 W/m²) and temperature (20 to 25°C) while maintaining the load constant (250 A). As shown in Figure 9b, there is significant improvement in the rise time and voltage dip and the V_{DC} has been maintained to 600 V which is the desired value. In comparison between Figure 10a and b, from 2 to 3 seconds solar irradiance dropped from 1000 to 750 W/m² and increased back to 1000 W/m² between 4 to 4.5 seconds while from 6 to 7 seconds temperature dropped from 25 to 20 °C and recovered between 7 to 8.5 seconds. Due to the presence of battery storage and buck-boost converter, the V_{DC} remained at 600 V in all these circumstances.

The performance of the designed converter under the hybrid system of solar PV, PMSG-based wind generator and with energy storage system was also investigated. The solar irradiance was varied from 750 to 1000 W/m²

from 2 to 4.5 seconds, temperature was varied from 20 to 25 °C from 6 to 8.5 seconds, and the wind speed was varied from 6.03 m/s to 13.48m/s. Figure 9c shows the variation of V_{DC} as output by the hybrid system under the discussed variations. During all variations, the load was kept constant. Despite the variation in solar irradiance, temperature and wind speed, there is a very slight variation in DC bus voltage. Besides, it can be observed that the V_{DC} has a maximum drop of approximately 0.67% which falls within the acceptable range.

**Performance of the DC-DC Converter Under Load Variation**

The performance of the designed converter under the hybrid system of solar PV, PMSG-based wind generator and energy storage system was also investigated under variation of load conditions. The load was varied from 0 to 260 A in a step of 70 A from 0 to 1.5 seconds, 140 A from 1.5 to 3.0 seconds, 190 A from 3.0 to 5.0 seconds and 260 A from 5.0 to 6.0 seconds (shown by Figure 9c). Figure 11 shows the variation of DC link voltage output by the hybrid system under the above load variations while maintaining solar irradiance, temperature, and wind speed at 1000 W/m², 25 °C and 13.48 m/s respectively. Despite the load variations, it can be observed that the V_{DC} falls within the acceptable range.
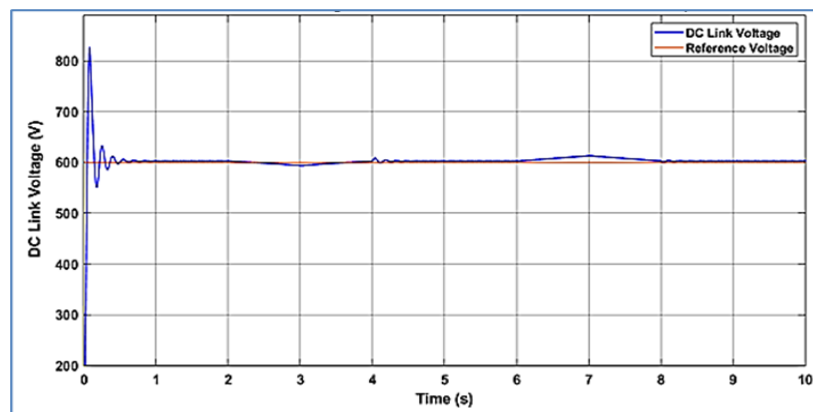
(a)
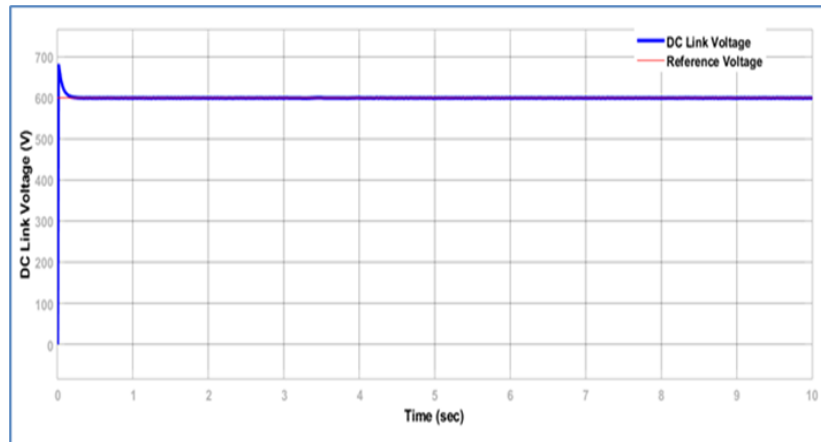
(b)
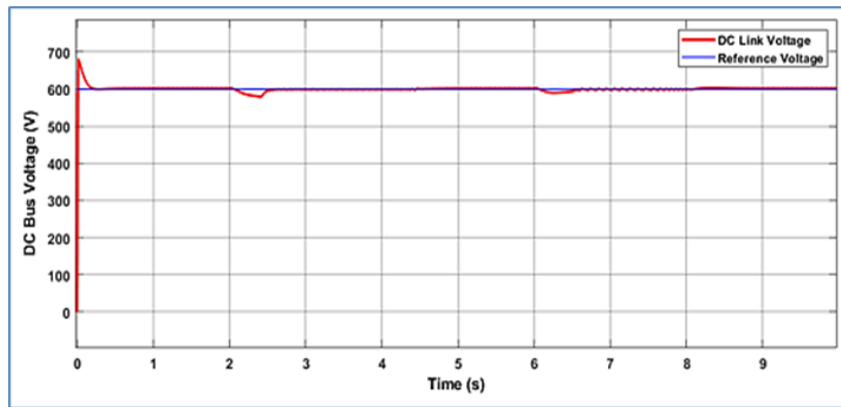
(c)

Figure 10: DC link voltage (a) under variation of solar irradiance, temperature and without energy storage system (b) under variation of solar irradiance, temperature and with energy storage system and (c) under variation of solar irradiance, temperature, and wind speed and without energy storage system.
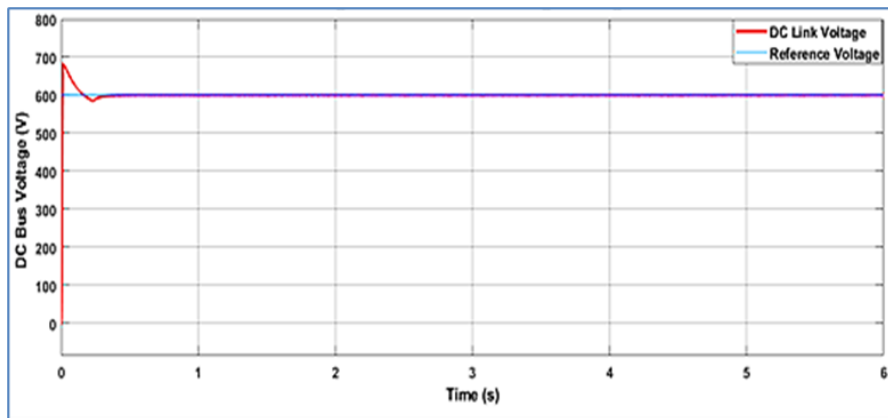

Figure 11: DC link voltage variations with solar PV, wind and energy storage system under variation of loads.

CONCLUSION

This study successfully designed a bidirectional buck-boost converter to increase and maintain the DC link bus voltage output by the hybrid solar PV with MPPT based algorithm, wind generator, and energy storage system under constant and variable load conditions. To design the bidirectional buck-boost converter, a one-year meteorological data (2020-2021) solar data and wind data at 50 m retrieved from NASA database were used. The targeted area for this study is Ikuza Island. The designed system was tested with varying solar irradiance (750 to 1000 W/m^2), temperature (20 to 25°C) and wind speed (150 to 157.5 radians/s) at constant load of 260 A while load variation involved varying the load current from 0 to 260 A at solar irradiance, temperature, and wind speed of 1000 W/m^2, 25 °C and 157.5 radians/s, respectively. The variations of DC link voltage at different load conditions were reported.

The findings revealed that the converter was able to maintain the DC link voltage at 600 V.

Under constant load of 260 A, temperature of 25°C and without energy storage system, variation in solar irradiance from 1000 to 750 W/m^2 led to drop in DC link voltage from 600 to 596 V. On the other hand, at a constant load of 260 A, solar irradiance of 1000 W/m^2 and without energy storage system, variation in temperature from 20 to 25°C led to increase in DC link voltage from 600 to 615 V. This superior performance was indicated by the DC link voltage which remained at 600 V in all these circumstances. Besides, when tested with the hybrid system of solar PV, PMSG-based wind generator and with energy storage system and varied from 750 to 1000 W/m^2, from 20 to 25 °C and from 150 radians/s to 157.5 radians/s, the DC link voltage showed the maximum drop of approximately 0.67% which

falls within the acceptable range. When varying the load from 0 to 260 A and while maintaining solar irradiance, temperature, and wind speed at 1000 W/m^2, 25 °C and 157.5 radians/s, respectively, it can be observed that the DC link voltage remains within the acceptable level.

The designed bidirectional buck-boost converter can integrate renewable energy sources with energy storage system, hence found to be an effective solution for remote and rural electrification. In addition, this research provides useful methodologies for the design and testing of bidirectional buck-boost converter in other countries where renewable electrification is found important.

ACKNOWLEDGEMENT

REFERENCES

Anish John Paul, M., Agees Kumar, C., & Jerusalin Carol, J. (2021). Investigation on extendable multiport DC–DC boost converter for hybrid renewable energy systems. *Automatika*, **62**(3–4), 486–502. https://doi.org/10.1080/00051144.2021.1985704

Badwawi, R. Al, Abusara, M., & Mallick, T. (2015). A Review of Hybrid Solar PV and Wind Energy System. *Smart Science*, **3**(3), 127–138. https://doi.org/10.1080/23080477.2015.11665647

Barone, G., Buonomano, A., Forzano, C., Giuzio, G. F., & Palombo, A. (2021). Supporting the Sustainable Energy Transition in the Canary Islands: Simulation and Optimization of Multiple Energy System Layouts and Economic Scenarios.

Frontiers in Sustainable Cities, **3**. https://doi.org/10.3389/frsc.2021.685525

Cabrera, P., Lund, H., & Carta, J. A. (2018). Smart renewable energy penetration strategies on islands: The case of Gran Canaria. *Energy*, **162**, 421–443. https://doi.org/10.1016/j.energy.2018.08.020

Chilumba, L., Mushi, A. T., & Mwinyiwiwa, B. M. M. (2023). Developing a Laptop Power Adaptor for 12 V and 24 V Solar PV Source. *11th International Conference on Power Electronics (ICPE 2023-ECCE Asia)*, 2157–2162.

Fungo, L. J., Mushi, A. T., & Msigwa, C. J. (2021, November 11). Grid Connected PV-Wind Energy System for Luxmanda Village in Tanzania. *The Third Annual Conference on Research and Inclusive Development*.

Garcia, R. G., Vergara, E. M., Paglinawan, C. C., Paglinawan, A. C., Lopez, J. F. V., Quilatan, J. P., Reyes, A. C. P., & Rivera, J. C. C. (2017). Design and implementation of a DC-DC boost converter for continuous hybrid power system. *2017IEEE 9th International Conference on Humanoid, Nanotechnology, Information Technology, Communication and Control, Environment and Management (HNICEM)*, 1–5. https://doi.org/10.1109/HNICEM.2017.8269547

GSA. (2023). *Global Solar Atlas: Kagera*. https://globalsolaratlas.info/map?s=-2.131542,31.773148&m=site&c=-2.13333,31.76667,11

Hajjaji, M., Mezghani, D., Cristofari, C., & Mami, A. (2022). Technical, Economic, and Intelligent Optimization for the Optimal Sizing of a Hybrid Renewable Energy System with a Multi Storage System on Remote Island in Tunisia. *Electronics*, **11**(20), 3261. https://doi.org/10.3390/electronics11203261

Irechukwu, M. E., & Mushi, A. T. (2020). Potential for Increased Rural Electrification Rate in Sub-Saharan Africa using SWER Power Distribution Networks. *Tanzania Journal of Engineering and Technology (Tanz. J. Engrg. Technol.)*, **39**(2). https://doi.org/10.52339/tjet.v39i2.707

Juma, M. I., Mwinyiwiwa, B. M. M., Msigwa, C. J., & Mushi, A. T. (2021a). Design of a hybrid energy system with energy storage for standalone DC microgrid application. *Energies*, **14**(18). https://doi.org/10.3390/en14185994

Juma, M., Mwinyiwiwa, B. M. M., Msigwa, C. J., & Mushi, A. T. (2021b). *Proposal Design of a Hybrid Solar PV-Wind-Battery Energy Storage for Standalone DC Microgrid Application*. https://doi.org/10.20944/preprints202108.0264.v1

Justo, J. J., & Mushi, A. T. (2020). Performance Analysis of Renewable Energy Resources in Rural Areas: A Case Study of Solar Energy. *Tanzania Journal of Engineering and Technology (Tanz. J. Engrg. Technol.)*, **39**(1), 1–12. https://doi.org/https://doi.org/10.52339/tjet.v39i1.514

Kalamaras, E., Belekoukia, M., Lin, Z., Xu, B., Wang, H., & Xuan, J. (2019). Techno-economic Assessment of a Hybrid Off-grid DC System for Combined Heat and Power Generation in Remote Islands. *Energy Procedia*, **158**, 6315–6320. https://doi.org/10.1016/j.egypro.2019.01.406

Kaldellis, J. K. (2021). Supporting the Clean Electrification for Remote Islands: The Case of the Greek Tilos Island. *Energies*, **14**(5), 1336. https://doi.org/10.3390/en14051336

Kapsali, M., & Anagnostopoulos, J. S. (2017). Investigating the role of local pumped-hydro energy storage in interconnected island grids with high wind power generation. *Renewable Energy*, **114**, 614–628. https://doi.org/10.1016/j.renene.2017.07.014

Khan, N. A., Sikder, A. K., & Saha, S. S. (2014). Optimal planning of off-grid solar-wind-

tidal hybrid energy system for sandwip island of Bangladesh. *2nd International Conference on Green Energy and Technology*, 41–44. https://doi.org/10.1109/ICGET.2014.6966658

LakshmanRao, P. S., Pearl Kurian, C., Singh, B. K., & Jyothi, A. V. (2014). Simulation and Control of DC/DC Converter for MPPT Based Hybrid PV/Wind Power System. *International Journal of Renewable Energy Research*, **4**(3).

Marcel, E. T., Mutale, J., & Mushi, A. T. (2021). Optimal Design of Hybrid Renewable Energy for Tanzania Rural Communities. *Tanzania Journal of Science*, **47**(5): 1716–1727. https://doi.org/10.4314/tjs.v47i5.19

Minja, M. N., & Mushi, A. T. (2022). Design and simulation of hybrid renewable energy sources for Mwanza International Airport. *7th International Conference on Mechanical and Industrial Engineering (MIE'2022)*, 5.

Minja, M. N., & Mushi, A. T. (2023). Design of International Airport Hybrid Renewable Energy System. *Tanzania Journal of Engineering and Technology*, **42**(1): 46–57. https://doi.org/10.52339/tjet.v42i1.887

NASA. (2023). *POWER | Data Access Viewer*. https://power.larc.nasa.gov/data-access-viewer/

Nyanda, E., Mushi, A., & Justo, J. (2022). Viability Analysis of Ubungo II Gas Power Plant Efficiency Improvement Using Co-Generation System. *Tanzania Journal of Engineering and Technology*, **41**(2): 158–170. https://doi.org/10.52339/tjet.v41i2.789

Raj, A., & Praveen, R. P. (2022). Highly efficient DC-DC boost converter implemented with improved MPPT algorithm for utility level photovoltaic applications. *Ain Shams Engineering Journal*, **13**(3): 101617. https://doi.org/10.1016/j.asej.2021.10.012

See, A. M. K., Mehranzamir, K., Rezania, S., Rahimi, N., Afrouzi, H. N., & Hassan, A. (2022). Techno-economic analysis of an off-grid hybrid system for a remote island in Malaysia: Malawali island, Sabah. *Renewable and Sustainable Energy Transition*, **2**, 100040. https://doi.org/10.1016/j.rset.2022.100040

Uthirasamy, R., Chinnaiyan, V. K., Vishnukumar, S., Karthick, A., Mohanavel, V., Subramaniam, U., & Muhibbullah, M. (2022). Design of Boosted Multilevel DC-DC Converter for Solar Photovoltaic System. *International Journal of Photoenergy*, *2022*, 1–23. https://doi.org/10.1155/2022/164847